

Deformable Resection Process Map for Intraoperative Cutting Guides

Megumi Nakao¹, *Member, IEEE*, Kojiro Taura² and Tetsuya Matsuda¹, *Member, IEEE*,

Abstract—In this paper, we will introduce the concept of deformable resection process mapping as a time-varying geometric guide for soft tissue tumor resection procedures. The deformable resection process map (RPM) estimates the local appearance of vascular structures after cuts as a novel guide. The RPM can be directly generated from patient-specific medical images using volumetric resampling techniques. Since user input of some cutting points is the only requirement for generating the RPM, the developed software will be directly available for clinical use to preview surgical procedures and intraoperative workflow management without time-consuming setups or additional workloads. We used the CT images of the patients with hepatic cancer for the experiments. The performance of our method in the shape representation for a curved cut surface was compared with that of conventional shape modeling methods.

I. INTRODUCTION

Virtual planning using preoperative computed tomography (CT) or magnetic resonance (MR) images enable quantitative, strategic planning of patient-specific cutting procedures for tumor resections [1]. The planned cutting path and virtual organ images are used as intraoperative cutting guides [2]. However, during surgery, rather than completely relying on the preoperative plans, the limited visible areas of vascular structures (e.g., optically visible or measured using imaging devices such as ultrasound), are commonly used for intraoperative decision-making. One reason to abandon the virtual plan is the shape of the virtual organs, which often differs from the deformed states of real organs. A deformed shape may occur because of altered physical conditions (e.g., air/blood pressure), push/pull manipulation, or cuts made during a surgical procedure. To perform evidence-based cutting and reduce surgical risks, the clinical requirements for estimating the visual appearance of such local features are increasing.

Although efforts have been made to provide multilateral anatomical information for navigating cutting procedures [3][4], the local appearance of vascular structures in the intraoperative deformed state has been omitted in planning/navigation software because modeling the effects of soft tissue cuts is difficult [5]. Intraoperative ultrasound (US) is used to detect tumors in a deformed organ. However, advanced imaging systems such as C-Arm and Open MRI are still only available in specialized operating rooms. Therefore, surgical navigation using preoperative CT/MRI images has gained attention even for deformed organs.

¹M. Nakao and T. Matsuda are with Graduate School of Informatics, Kyoto University, Kyoto, 606-8501, JAPAN (e-mail: megumi@i.kyoto-u.ac.jp, tetsu@i.kyoto-u.ac.jp). ²K. Taura is with Dept. of Hepato-Biliary-Pancreatic and Transplant Surgery, Kyoto University Hospital, Kyoto, 606-8507, JAPAN.

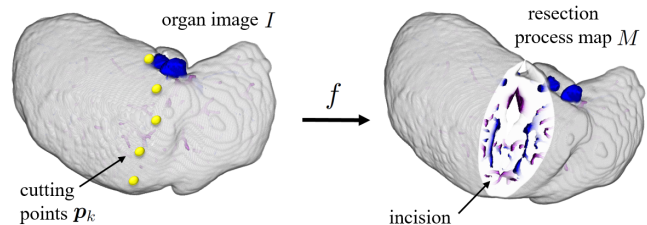


Fig. 1. Deformable resection process map (RPM) and direct generation from medical images

Despite the interest among surgeons and researchers, a CT-based estimator that represents the intraoperative deformed state of organs has not received much attention compared to intraoperative measurement and registration methods. Our motivation for this research was to address this clinical need and to present a time-varying local map of the resection process. To the best of our knowledge, a progressive, deformable representation of the resection guide and direct generation from patient-specific CT images has not been achieved in the medical image computing literature. Although some studies, including our previous work, developed volumetric image manipulation methods for patient-specific images [6][7], the clinical applicability of generation of the complex curved shapes of a resection path has not been addressed.

In this paper, we will introduce the deformable resection process map (RPM) for estimating the local appearance of vascular structures after cuts as a novel guide for soft tissue tumor resection procedures. The deformable RPM is a geometrical estimator that provides a time-varying local map based on the deformed geometry of the organs. Unlike static virtual-reality-based training simulators for cutting/ablation procedures, we designed a set of algorithms to provide a semi-automatic software framework tuned for planning/navigation. The experiments show that the RPM can represent a variety of curved resection paths and provides a high-quality visual map for preoperative/intraoperative use, which can be directly generated from patient-specific medical images.

II. DEFORMABLE RESECTION PROCESS MAP

A. Problem Definition

Figure 1 shows a brief description of the problem definition in the proposed RPM M . To achieve semi-automatic generation of the RPM from medical images, we newly designed an objective function $f(I, p_k)$ that computes M with the smooth cutting path S from the segmented organ image I and a set of cutting points p_k (Eq.1).

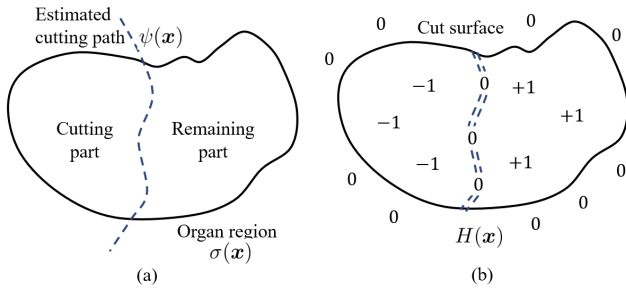


Fig. 2. Shape function describing discontinuity in 3D images

$$M = f(I, \mathbf{p}_k) \quad (1)$$

Obviously, the initial CT/MRI images are spatially continuous and the target map represents a partially discontinuous organ image deformed by incision. In order to approach this, first, as a background process, the three-dimensional organ region is sparsely sampled and a proxy geometry bounded by the reference cutting path ψ_0 and enclosing the sampled points is generated. The proxy geometry can be described using a tetrahedral mesh [7][8]. When some cutting points \mathbf{p}_k are plotted on the vascular structures or on the organ surface, the vertices of the proxy geometry are relocated using a quadratic minimization function, which is designed to preserve the local shape consistency of the given points \mathbf{p}_k and the reference cutting path ψ_0 . The cutting points can be manually supplied by the user or extracted from the boundary of segmented blood vessel regions. Based on the time-varying least squares cutting path ψ^* , the RPM is visualized in a deformed volumetrically-rendered organ image.

The computation methods for the proxy geometry with a reference cutting path is described in Section II-B, and algorithms for generating the least square cutting path are explained in Section II-C.

B. Proxy Geometry with Reference Cutting Path

The reference cutting path ψ_0 is introduced to model prior knowledge for dividing an organ into two parts in cutting procedures. To represent ψ_0 , we define $\sigma(\mathbf{x})$ and $\psi(\mathbf{x}) : \mathbb{R}^3 \rightarrow \mathbb{R}$ as volume indicator functions that represent the organ and the cutting region, respectively. Here as illustrated in Fig. 2(a), we define that a point $\mathbf{x} \in \mathbb{R}^3$ is inside the organ if $\sigma(\mathbf{x}) < 0$, and outside the organ if $\sigma(\mathbf{x}) > 0$. Similarly, a point \mathbf{x} is inside the cutting region if $\psi(\mathbf{x}) > 0$. The tumor as the resection target is also located in the cutting region. Then, the set of points \mathbf{x} , where $\psi(\mathbf{x}) = 0$, forms the cutting path, and specifically represents a cut surface S created inside the object if $\psi(\mathbf{x}) = 0$ and $\sigma(\mathbf{x}) < 0$. When the object is divided into two parts by $\psi(\mathbf{x}) = 0$, the set of points where $\sigma(\mathbf{x}) < 0$ and $\psi(\mathbf{x}) > 0$ represent the remaining part and the other points with $\sigma(\mathbf{x}) < 0$ and $\psi(\mathbf{x}) < 0$ represent the cutting part.

To formulate the above geometrical properties, we will introduce the novel shape function $H(\mathbf{x}) : \mathbb{R}^3 \rightarrow \mathbb{R}$ that

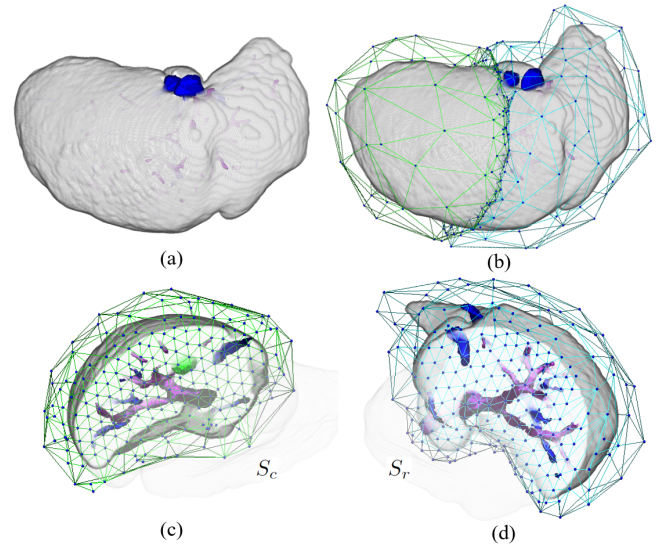


Fig. 3. Initial proxy geometry with reference cut surfaces, (a) segmented liver volume, (b) initialized proxy geometry, (c) reference cut surface of cutting part S_c and (d) reference cut surface of cutting part S_r .

describes discontinuity in a volumetric space when dividing an object. It is defined by

$$H(\mathbf{x}) = \begin{cases} +1 & \text{if } \sigma(\mathbf{x}) < 0 \text{ and } \psi(\mathbf{x}) > 0 \\ 0 & \text{if } \sigma(\mathbf{x}) \geq 0 \text{ or } \psi(\mathbf{x}) = 0 \\ -1 & \text{if } \sigma(\mathbf{x}) < 0 \text{ and } \psi(\mathbf{x}) < 0 \end{cases} \quad (2)$$

where $H(\mathbf{x})$ is the generalized form of the Heaviside function. The isosurface $H(\mathbf{x}) = 0$ forms the boundary of the object with the cut surface, i.e., the interface between the remaining part and the cutting part. We note that this description is based on the conventional indicator function on an implicit surface [9], and its application to volumetric image cutting.

$H(\mathbf{x})$ is discretely sampled by a multi-material volumetric label consisting of three regions: the remaining region R_r , cutting region R_c and cutting path R_p (see Fig. 2(b)). R_p can be computed using

$$R_p = D(R_c, r) \wedge D(R_r, r) \quad (3)$$

where D is morphological dilation function of a binary image and r is the radius in the dilation operation, with $r = 2$ being used in our case. The initial proxy geometry with the reference cut surfaces: S_r on the remaining part and S_c on the cutting part are then generated from this multi-material label using the marching cubes method. Figure 3 shows an example of the proxy geometry, which has two parts facing each other at the reference cut surfaces.

C. Least Squares Cutting Path

Our interest lies in generating the cut surface S that satisfies the positional constraints of sparsely distributed cutting points \mathbf{p}_k . The curved shape of S can be more complex as the number of indicated cutting points increases.

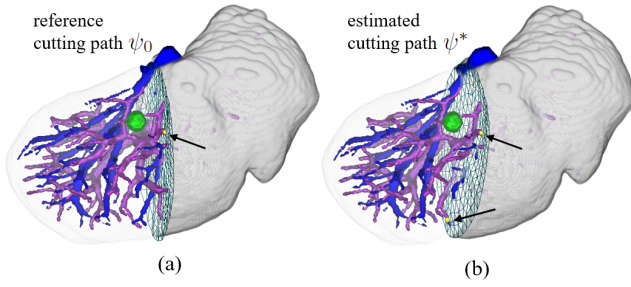


Fig. 4. Progressive geometry update, (a) reference cutting path ψ_0 and (b) estimated least squares cutting path ψ^* locally fit to the supplied cutting points.

However, complete reconstruction of the proxy geometry requires a large computation cost for mesh generation and the setup of a stiffness matrix used for elastic deformation.

In order to approach this problem, when some cutting points \mathbf{p}_k are given on the vascular structures or on the organ surface, the vertices $V = \{\mathbf{v}_0, \mathbf{v}_1, \dots, \mathbf{v}_{n-1}\}$ of the proxy geometry are relocated while preserving the local shape consistency of the given points \mathbf{p}_k , the reference cutting path ψ_0 and the proxy geometry. Figure 4 briefly shows the outline of the methods. This update of the proxy geometry is performed by preserving the discrete Laplacian [10], and the estimated cutting path ψ^* is locally fit to the cutting points in a least squares manner, as defined in Eq. (4).

$$\hat{V} = \operatorname{argmin}_V \sum_{i=0}^{n-1} \|L(\hat{\mathbf{v}}_i) - L(\mathbf{v}_i)\|^2 + \sum_{i=0}^{n-1} \|\mathbf{p}_i - \mathbf{v}_i\|^2 \quad (4)$$

$$L(\mathbf{v}_i) = \sum_{j \in N(\mathbf{v}_i)} w_{ij}(\mathbf{v}_i - \mathbf{v}_j) \quad (5)$$

where $L(\cdot)$ is a Laplacian operator, \mathbf{v}_i is the initial position, and $\hat{\mathbf{v}}_i$ is the target position to be solved. \mathbf{p}_i is the positional constraint for the i th vertex, and $N(\mathbf{v}_i)$ is the set of adjacent vertex indexes of the i th vertex. The Laplacian vector at the i th vertex can be computed using a weight parameter w_{ij} , as shown in Eq. (5).

This approach estimates the cutting path using the given cutting points as geometrical constraints and produces a time-varying local map of vascular structures with a progressive deformable representation. We note that the geometry update is performed by Laplacian-based surface registration without relying on vertex addition or mesh subdivision. This scheme enables fast and real-time computation while handling the time-varying geometry of the cutting path. This concept addresses the technical issues discussed in [2] and formulates the RPM as a generalized computation framework that can be applied to non-anatomical cutting paths by improving volumetric resampling techniques [8].

D. Deformation and Visualization

When cutting points are indicated on the organ surface or vessels, the RPM is updated and the virtual organ is deformed

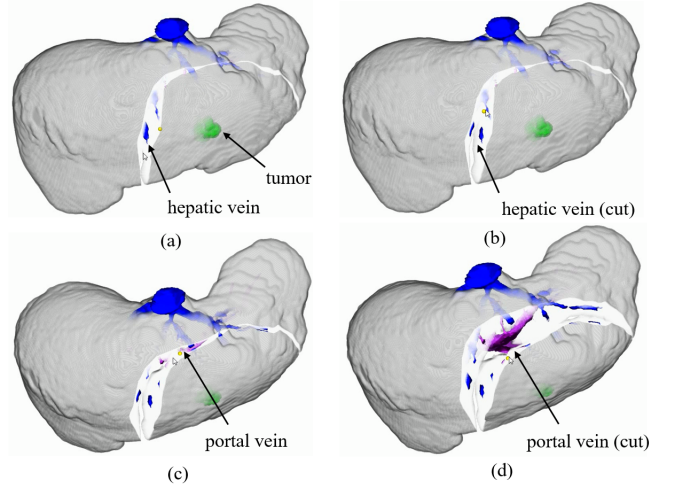


Fig. 5. Time-series representation of the deformable RPM.

by applying an external force to the cut surfaces S_c and S_r . The discontinuous deformation around the cutting path is computed in the proxy mesh, and the final image of the RPM is generated through volume rendering of tetrahedral grids [6][8]. Since the proxy geometry is formed by a tetrahedral mesh, finite element models can be directly applied to represent elastic deformation. When the user manipulates the volume, current vertices \hat{V} are displaced to V^* through mesh deformation. Then, our framework renders the deformed volume using the new coordinates of V^* , incorporating the intensity of the 3D CT image I . The vascular structures in the deformed body are linearly interpolated and visualized volumetrically in the proxy geometry.

III. EXPERIMENTS AND RESULTS

We implemented the proposed deformable RPM framework using Visual C/C++, OpenGL and OpenGL Shading Language (GLSL). The experiments were designed as a retrospective user study involving surgeons in the Department of Hepato-biliary Pancreatic and Transplant Surgery in Kyoto University Hospital. Twenty-one CT datasets for hepatectomy were applied to the developed software framework, and the RPMs were generated in a variety of the deformed states. The CT slice images were first re-sampled as regularized volume data with 256^3 voxels, and the liver region I was manually extracted. To do this, we assumed intraoperative use of the RPM and tried to reproduce the cutting paths conducted in previous surgeries. Based on the typical shapes of the cutting paths, three primitive surface types, plane, quadric and hemispherical, were used to generate the initial reference cutting path ψ_0 . Since we did not target a physically accurate simulation of elastic behavior, but instead targeted the generation of a deformable map for intraoperative guidance, the Young's modulus and Poisson's ratio were uniformly set at 100kPa and 0.4, respectively for the proxy mesh. In this paper, due to the limitations of space, we will report only three typical instances that have different cutting path shapes.

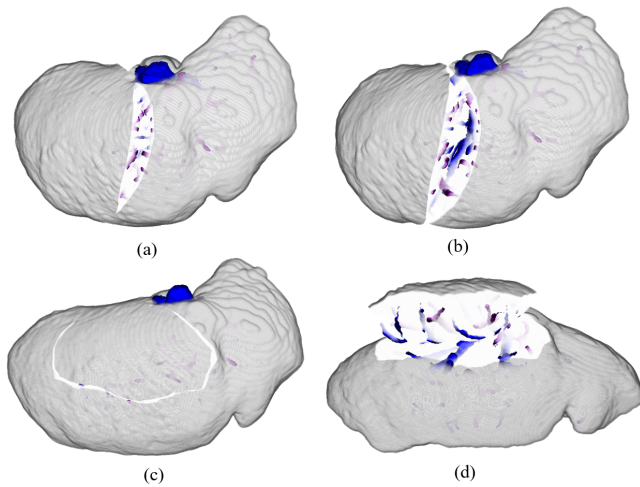


Fig. 6. RPMs for two types of cutting procedures.

Figure 5 demonstrates a time-series representation of the resection process map generated from a single CT image set. As the procedure progressed, an updated local appearance was rendered of anatomical structures such as a tumor, a hepatic vein, and a portal vein in the deformed organ, and a distribution of the vascular structures already split by cutting. The estimated visual appearance of the vessels at most the deepest points of incisions are key structures for decision-making on next cutting directions. Figure 6 shows the deformed RPMs for two types of cutting procedures generated from another single CT image set. The plane and the quadric reference cutting paths were used, respectively. Based on the supplied cutting points, the cut surface was locally fit to the estimated curved paths. These results show that interactive mesh adaptation coupling with elastic deformation has good potential for generating an RPM while satisfying clinical needs for a variety of complex cutting paths.

In addition to shape representation, real-time performance is a key for clinical use. In case of the three types of cutting procedures in Fig. 5 and in Fig. 6, we measured the computation time for generating a geometrical update of the cutting path, elastic deformation and volume rendering of the deformed organ. In the experiments, we used general-purpose computers with graphic processing units (CPU: 3.5 GHz, Memory: 8 GB, GPU: NVIDIA GeForce 780). The average computation time for each process was 17.9 msec for geometrical update, 17.4 msec for elastic deformation, and 15.9 msec for rendering deformed volumes. We confirmed that an interactive update of the RPM, including deformation computation, was possible greater than 15 frames/s.

IV. DISCUSSION

Regarding comparison to past approaches for intraoperative guidance, Lamata et al. [2] provided a resection map with cross-sectional images of vascular structures. However, as discussed in [2], to cope with organ deformation was a problem. In recent work on deformation mapping [6], the reconstructed cut surfaces were still limited to primitive

shapes. The obtained results address these issues and volumetrically visualize a variety of cuts in a deformed state. Since the only required user interaction is to input some cutting points to generate the RPM from medical images, the developed software will be directly available for clinical use to preview surgical procedures and in intraoperative workflow management without requiring a time-consuming setup or additional workloads.

V. CONCLUSIONS

We introduced deformable RPM as a time-varying geometric guide for cutting procedures. The algorithmic design for semi-automatic generation from medical images was described here. The obtained visualization results demonstrate the preliminary performance of the presented methods. A quantitative evaluation of the generated cut surface geometry and clinical validation will be our future work.

ACKNOWLEDGMENT

This research was supported by JSPS Grant-in-Aid for Scientific Research (B) (15H03032) and the Center of Innovation (COI) Program of the Japan Science and Technology Agency (JST).

REFERENCES

- [1] Y. Mise, K. Tani, T. Aoki, Y. Sakamoto, K. Hasegawa, Y. Sugawara, et al., "Virtual liver resection: computer-assisted operation planning using a three-dimensional liver representation," *Journal of Hepato-Biliary-Pancreatic Sciences*, vol. 20, no. 2, pp. 157-164, 2013.
- [2] P. Lamata, A. Jalote-Parmar, F. Lamata, and J. Declerck, "The resection map, a proposal for intraoperative hepatectomy guidance," *International Journal of Computer Assisted Radiology and Surgery*, vol. 3, pp. 299-306, 2008.
- [3] J. Hallet, B. Gayet, A. Tsung, G. Wakabayashi, and P. Pessaux, "Systematic review of the use of pre-operative simulation and navigation for hepatectomy: current status and future perspectives," *J Hepatobiliary Pancreat Sci*, vol. 22, no. 5, pp. 353-62, 2015.
- [4] M. Sato, M. Omasa, F. S. Chen, T. Sato, M. Sonobe, T. Bando, et al., "Use of virtual assisted lung mapping (VAL-MAP), a bronchoscopic multispot dye-marking technique using virtual images, for precise navigation of thoracoscopic sublobar lung resection," *Journal of Thoracic and Cardiovascular Surgery*, vol. 147, no. 6, pp. 1813-1819, 2014.
- [5] M. Nakao and K. Minato, "Physics-based interactive volume manipulation for sharing surgical process," *IEEE Trans. on Information Technology in Biomedicine*, Vol.14, No. 3, pp. 809-816, 2010.
- [6] A. Rodriguez Aguilera, A. Leon Salas, D. Martin Perandres, and M. A. Otaduy, "A parallel resampling method for interactive deformation of volumetric models," *Computers & Graphics*, vol. 53, Part B, pp. 147-155, 2015.
- [7] M. Nakao, Y. Oda, K. Taura, and K. Minato, "Direct volume manipulation for visualizing intraoperative liver resection process," *Computer Methods and Programs in Biomedicine*, vol. 113, no. 3, pp. 725-735, 2014.
- [8] K. W. C. Hung, M. Nakao, K. Yoshimura, and K. Minato, "Background-incorporated volumetric model for patient-specific surgical simulation: a segmentation-free, modeling-free framework," *International Journal of Computer Assisted Radiology and Surgery*, vol. 6, no. 1, pp. 35-45, 2011.
- [9] M. Meyer, R. Whitaker, R. M. Kirby, C. Ledergerber, and H. Pfister, "Particle-based sampling and meshing of surfaces in multimaterial volumes," *IEEE Transactions on Visualization and Computer Graphics*, vol. 14, no. 6, pp. 1539-1546, 2008.
- [10] O. Sorkine, D. Cohen-Or, Y. Lipman, M. Alexa, C. Rossl, and H. P. Seidel, "Laplacian surface editing," *Proc. of the Eurographics/ACM SIGGRAPH symposium on Geometry Processing*, pp. 175-184, 2004.